

Flame-based Aerosol Synthesis of Metal Nanoparticles and Supported-Metal Nanostructures

Shuo Liu and Mark T. Swihart*

*Department of Chemical and Biological Engineering, University at Buffalo,
The State University of New York, Buffalo, NY 14260, USA

ABSTRACT

Commercialization of inorganic nanomaterials is often limited by scale-up. Our group developed a unique flame-based aerosol process for scalable, continuous, and low-cost production of various nanomaterials, the High Temperature Reducing Jet (HTRJ) Reactor. Over the past decade, a wide range of inorganic nanoparticles has been produced by this process, including metal and alloy nanomaterials (Ag, Cu-Ni, Cu-Ag-Sn, etc), dense, hollow, and porous ceramic materials (Al_2O_3 , SiO_2 , etc), and supported-metal nanomaterials (Ni/MgO, $\text{CrO}_x/\text{SiO}_2$, Pd/graphene, etc). Based on their specific properties, these materials have broad utility and excellent performance in energy and environmental applications, such as printed electronics, thermal insulation materials, catalysis, and sensors.

Keywords: Flame aerosol process, nanoparticles, energy applications, scalable production

1 HTRJ FLAME AEROSOL REACTOR

Flame aerosol technology, the most common method for industrial production of low cost aerosol materials, such as carbon black and fumed silica, has been extended to produce a much broader range of inorganic nanomaterials over the past twenty years. Ten years ago, Scharmach et al. [1] designed and built a new type of flame reactor for synthesizing metal nanoparticles, which they called the HTRJ reactor, as shown in **Figure 1**. Using an aqueous precursor solution, the HTRJ reactor belongs to FASP (Flame Assisted Spray Pyrolysis) category of methods. It uses a $\text{H}_2\text{-O}_2$ flame to supply the energy required for nanoparticle formation. In the reaction process, the excess H_2 , N_2 , and combustion product vapor pass through a converging-diverging nozzle, forming a supersonic hot gas flow. Meanwhile, a liquid precursor is injected into the throat of the nozzle, where it is instantly atomized by the hot gas jet. In the reaction chamber, the precursor droplets evaporate and decompose, and the inorganic solutes undergo nucleation, growth, and aggregation processes to form nanoparticles, followed by quenching with nitrogen at the reactor outlet and collection on a filter membrane. Conventional flame-spray aerosol processes use a combustible organic solvent as precursor and the particle forms in the flame. In contrast, the HTRJ process separates the flame and particle formation into different regions, which

allows use of a low enthalpy aqueous precursor instead of an organic solvent with metalorganic precursors, which greatly decreases feed costs. More importantly, this separation enables production of metal nanomaterials, because many noble and transition metal oxides can be reduced by H_2 in the reaction chamber. Elements that can be reduced by H_2 in the presence of H_2O form as metals, while those that can be oxidized by H_2O in the presence of H_2 form as oxides. Also, it provides a lower reaction temperature (400~800 °C) compared to tradition flame aerosol processes (often above 2000°C), which opens up new possibilities for controlling internal nanoparticle structure and greatly extends the range of materials that can be produced.

Generally, particle formation mechanisms in spray-based aerosol processes can be divided into gas-to-particle and droplet-to-particle routes. [2] For a gas-to-particle route, the droplets and precursors fully evaporate, and the product nucleates, grows, and aggregates from a supersaturated vapor. In contrast, the product forms in the liquid phase in the droplet-to-particle route, and each droplet yields one product particle. During the evaporation process, the solute concentration increases. The evaporation happens on the droplet surface, and the whole process is very fast (~50 ms in the HTRJ process) which allows limited solute diffusion, resulting in a higher concentration at the droplet surface where solvent evaporation occurs. Therefore, the product nucleates on the droplet surface and then grows towards center, finally forming a hollow structure after all the solvent disappear. Sometimes a solid particle forms when the precursor concentration is high or the melting point of the product material is low. Droplet-to-particle conversion often produces larger hollow or solid particles with a diameter of hundreds of nanometers, whereas gas-to-particle conversion usually produces solid particles with diameters of tens of nanometers. In the HTRJ flame process, both gas-to-particle and droplet-to-particle routes are possible, depending upon multiple factors, such as material composition, reaction temperature, and precursor concentration. Many metals produced from nitrate precursors follow the gas-to-particle mechanism to form nanoparticles, while many ceramic materials follow a droplet-to-particle route to form a hollow structured nanoshell with a larger diameter, but there are exceptions for both categories of material.

The HTRJ reactor can produce inorganic materials with different composition, structure, and morphology by control of reaction parameters. To date, various metal nanoparticles,

ceramic materials, and supported nanostructures have been synthesized in the HTRJ reactor. These materials, especially the ceramic-supported metal nanoparticle category, have great application potential in energy-related fields.

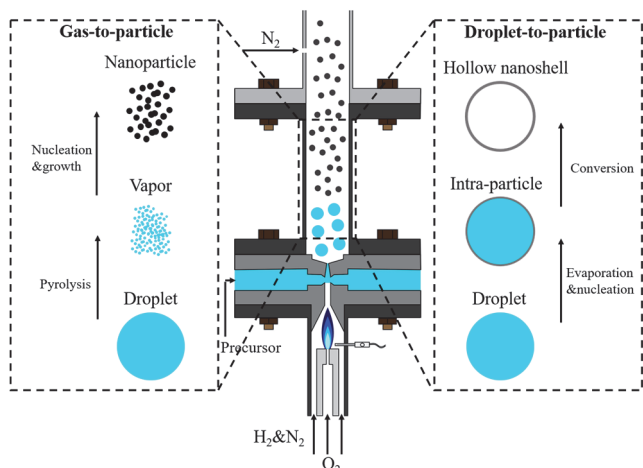


Figure 1. Configuration and particle formation mechanism of HTRJ flame aerosol reactor.

2 METAL NANOPARTICLES

Synthesis of metal nanoparticles was the initial purpose of the HTRJ flame reactor. Cu nanoparticles were the first nanomaterial produced by it, from a precursor of copper formate. [1] In the reaction process, copper formate decomposed to CuO and CO. The CuO was reduced to Cu, and CO also could be reduced by H₂, forming carbon that deposited on the Cu surface, as shown in **Figure 2(a)**. The *in-situ* carbon coating could prevent Cu nanoparticle aggregation and oxidation. Carbon-encapsulated Ag nanoparticles were prepared by a similar method. [3]

In the next few years, the HTRJ reactor was devoted to producing various conductive metal nanoparticles. For example, bimetallic Cu-Ag core-shell structured nanoparticles (**Figure 2(b)**) were developed and exhibited an abrupt transition from a low conductivity of $\sim 10^{-2}$ S/m to a high conductivity of $\sim 10^5$ S/m between 30 wt.% and 40 wt.% silver content. [4] Later, Cu-Ni, [5] Sn-Ag-Cu, [6] and Ni-Ag nanoparticles (**Figure 2(c)**) [7] were produced for potential applications in electrically-conductive films, coatings, and inks for printed electronics.

The surface modification of metal nanoparticles was achieved by addition of an *in-situ* functionalization device to the N₂ quenching region of the process, which could allow direct production of surface-modified particles. For example, octylamine was sprayed into the quench section of the HTRJ reactor to cap Pd-Cu alloy nanoparticles (**Figure 2(d)**) in the gas phase, loading the amine-containing ligands on the nanoparticle surface and making them directly dispersible in non-polar organic solvents.

Generally, nanoparticles of many transition metal elements can be reduced by hydrogen in the HTRJ flame reactor, to form metal nanoparticles with small diameters of 5~20 nm via a gas-to-particle route. A key advantage of the method is that complete conversion of precursors to products allows easy control of the product nanoparticle composition.

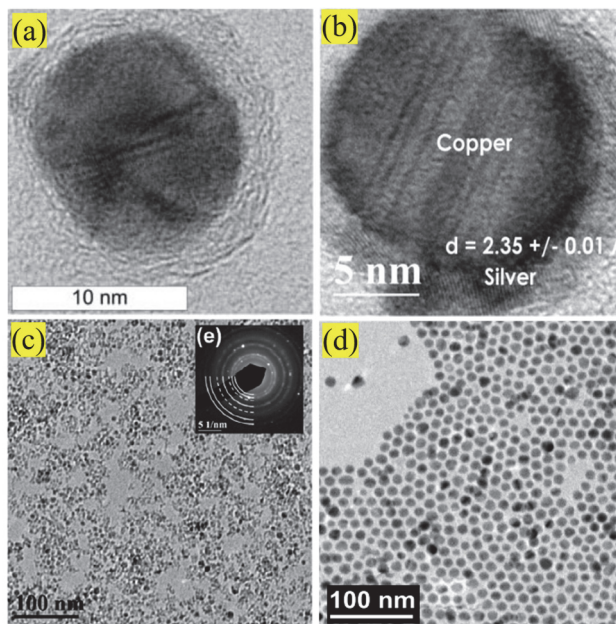


Figure 2. HTRJ flame reactor synthesized (a) C-coated Cu, (b) Cu-Ag, (c) Ni-Ag, and (d) Pd-Cu nanoparticles.

3 CERAMIC MATERIALS

The relatively low temperature of the particle formation process, relative to other flame reactors and to the melting points of ceramic materials, favors production of hollow ceramic materials via a droplet-to-particle route without using any organic template. A representative material of this category is hollow alumina nanoshells, as shown in **Figure 3(a)**, which exhibited a shell thickness below 10 nm and an average diameter of 181 nm. [8] This hollow alumina also exhibits low crystallinity and high thermal stability, maintaining the hollow structure at up to 1200 °C. As an aerosol ceramic material, the hollow alumina has a natural low thermal conductivity of 0.026 W/(m K). For better use of it as thermal insulation material, we assembled the hollow alumina nanoshells into a composite with commercial fiberglass insulation matrix by simple mechanical methods, to produce a high performance thermal insulation composite with a low thermal conductivity of 0.028 W/(m K) and robust mechanical properties. Many other hollow nanomaterials were produced by the same process, including SiO₂, ZrO₂, Co₂O₃, and Ga₂O₃, indicating the generality of the HTRJ flame process for synthesis of hollow nanoshells.

We also found the opportunity to prepare high porosity mesoporous silica in the HTRJ reactor, by an evaporation-driven self-assembly process in the droplet-to-particle

process, as shown in **Figure 3(b)**. In this process, a liquid precursor solution including TEOS (silica precursor), CTAB (surfactant), water, ethanol, and a small amount of hydrochloric acid was injected into the HTRJ reactor. During the particle formation process, the CTAB self-assembled into cylindrical micelles, and the TEOS was adsorbed on the micelle surface, forming an intermediate product. High porosity and surface area were generated by removal of the micelle template by calcination. The overall structure was also hollow, similar to alumina. The silica porosity, morphology, and density were tuned by controlling the flame reaction parameters, such as the precursor composition, reaction temperature, and gas flow rate. BET surface areas of this mesoporous reached $1030 \text{ m}^2/\text{g}$, with a pore volume of $0.75 \text{ cm}^3/\text{g}$ and average pore size of 3.54 nm . Densities of this hollow porous material could be as low as $0.015 \text{ g}/\text{cm}^3$. As an aerosol ceramic material, such a hollow structured mesoporous silica exhibits a better thermal insulation performance than the hollow alumina. Moreover, its high surface area and adsorption capacity have many other uses, *e.g.*, as a catalyst support, drug carrier, or adsorbent.

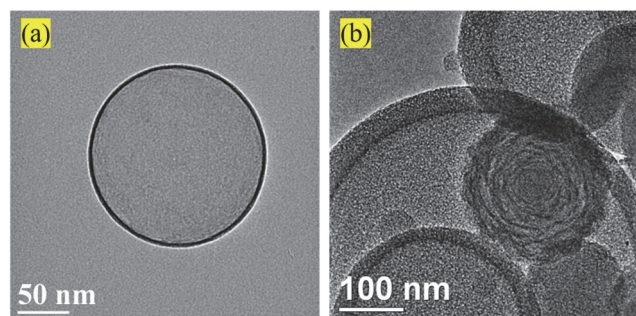


Figure 3. (a) HTRJ flame reactor synthesized hollow alumina nanoshell; (b) HTRJ flame reactor synthesized hollow structured mesoporous silica.

4 SUPPORTED METAL NANOSTRUCTURES

Supported metal nanostructures have crucial applications in energy-related fields. For example, most the heterogeneous catalysts are supported nanomaterials, in which the metal (or metal oxide) nanoparticles provide catalytically active sites, and the support materials provide good dispersion of the active nanoparticles and may add adsorption capacity for the reactants. The HTRJ reactor can achieve this structure in a single step, opening up new applications in energy and environmental fields.

The dry reforming of methane (DRM) reaction converts two greenhouse gases, CH_4 and CO_2 , into syngas (H_2 and CO), which is suitable to produce liquid fuels by the Fischer-Tropsch process. Ni is the most common active catalyst for this reaction, and ceramic materials, such as MgO , ZrO_2 , Al_2O_3 , and SiO_2 are the common supports. The HTRJ flame reactor can produce high activity and stability catalysts for the DRM reaction in a single step, using an aqueous

precursor solution of inorganic nitrate salts. To date, we have successfully synthesized Ni/MgO , Ni/ZrO_2 , $\text{Ni}/\text{Al}_2\text{O}_3$, Ni/CeO_2 , $\text{Ni}/\text{La}_2\text{O}_3$, and Ni/SiO_2 catalysts. [9] Among them, the Ni/MgO and Ni/ZrO_2 have outstanding catalytic performance for this reaction. TEM images of these materials are shown in **Figure 4(a)** and **(b)**. For the Ni/MgO catalyst, Ni and Mg follow the gas-to-particle route to form a solid solution structure with an average particle size below 20 nm. In contrast, in the Ni/ZrO_2 catalyst, the Ni and Zr follow the droplet-to-particle route to form a hollow structure. Despite the difference in particle formation mechanism and final morphology, both provided much better performance than the same catalysts prepared by traditional wet-impregnation or co-precipitation methods, stably providing more than 90% CH_4 conversion at $800 \text{ }^\circ\text{C}$, without excessive coking, sintering, or other deactivation.

Figure 4(c) shows a mesoporous silica supported CrO_3 nanocatalyst prepared in the HTRJ reactor for CO_2 oxidative dehydrogenation of propane with a BET surface area of $587 \text{ m}^2/\text{g}$. The mesoporous silica was formed by the self-assembly process, and the CrO_3 active sites was formed by a gas-to-particle route. This combination produced very small CrO_3 nanoparticles on the silica surface, which provided a 45% initial propane conversion due to the good dispersion. However, the propane conversion decreased to 15% after 10 h reaction at $600 \text{ }^\circ\text{C}$. The major reason for the deactivation is sintering of CrO_3 nanoparticles. The amorphous SiO_2 does not provide strong interactions with CrO_3 that could limit its mobility and prevent sintering. A key advantage of this catalyst is that it can retained 95% propylene selectivity even as it deactivated.

The HTRJ reactor also provides a general approach for synthesizing multicomponent metal-decorated crumpled reduced graphene oxide nanocomposites, incorporating a diverse array of transition metal and noble metal nanoparticles, like Co, Ni, Fe, and Pd, as well as various alloys including CoPd -, CoNi -, CoPdNi -, and CoNiFe . [10] Generally, the average diameter of these metal and alloy nanoparticles were 5 nm or less. Among these materials, the graphene-supported Pd nanostructure is a promising H_2 sensor material, as shown in **Figure 4(d)**. [11] A sensor using it was effective over a wide range H_2 concentrations of 0.0025–2% with short response and recovery times. At 2% H_2 , the response value, response time, and recovery time were 14.8%, 73 s, and 126 s, respectively. Also, it was suitable for both humid and dry environment with good stability and restorability.

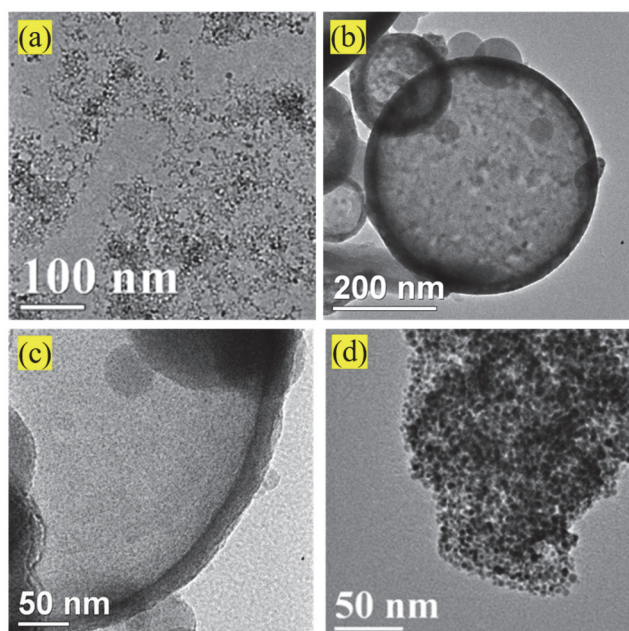


Figure 4. (a) Ni/MgO and (b) Ni/ZrO₂ catalysts for dry reforming of methane; (c) CrO₃/SiO₂ catalyst for CO₂ oxidative dehydrogenation of propane; (d) Pd/graphene for H₂ sensor.

5 CONCLUSION AND OUTLOOK

We present a unique vapor-phase synthesis method for scalable production of various metal nanoparticles, ceramic materials, and supported metal nanoparticles with potential applications in numerous energy-related applications. The HTRJ flame process can flexibly tailor the composition, morphology, and structure of materials towards targeted purposes. The development of hollow and porous ceramic-supported metal (or metal oxide) nanoparticles for catalysis is a major emerging direction in this research. We will design low-cost high-performance nanocatalysts to address key energy and environmental challenges facing humanity, such as climate change and clean energy utilization. Meanwhile, we will explore new possibilities of the HTRJ reactor, like aerosol synthesis of metal organic frameworks and high entropy alloys. Ultimately, a pilot scale HTRJ reactor might be developed for larger-scale production of the many materials we have developed in the lab.

REFERENCES

- [1] W.J. Scharmach, R.D. Buchner, V. Papavassiliou, P. Pacouloute, M.T. Swihart, A High-Temperature Reducing Jet Reactor for Flame-Based Metal Nanoparticle Production, *Aerosol Sci. Technol.* 44 (2010) 1083-1088.
- [2] S. Liu, M.M. Mohammadi, M.T. Swihart, Fundamentals and recent applications of catalyst synthesis using flame aerosol technology, *Chem. Eng. J.* 405 (2021).

- [3] W.J. Scharmach, M.K. Sharma, R.D. Buchner, V. Papavassiliou, G.N. Vajani, M.T. Swihart, Amorphous Carbon Encapsulation of Metal Aerosol Nanoparticles for Improved Collection and Prevention of Oxidation, *AIChE J.* 59 (2013) 4116-4123.
- [4] M.K. Sharma, R.D. Buchner, W.J. Scharmach, V. Papavassiliou, M.T. Swihart, Creating Conductive Copper-Silver Bimetallic Nanostructured Coatings Using a High Temperature Reducing Jet Aerosol Reactor, *Aerosol Sci. Technol.* 47 (2013) 858-866.
- [5] M.K. Sharma, D. Qi, R.D. Buchner, W.J. Scharmach, V. Papavassiliou, M.T. Swihart, Flame-driven Aerosol Synthesis of Copper-Nickel Nanopowders and Conductive Nanoparticle Films, *ACS Appl. Mater. Interfaces* 6 (2014) 13542-13551.
- [6] M.K. Sharma, D. Qi, R.D. Buchner, M.T. Swihart, W.J. Scharmach, V. Papavassiliou, Flame synthesis of mixed tin-silver-copper nanopowders and conductive coatings, *AIChE J.* 62 (2016) 408-414.
- [7] M.M. Mohammadi, S.S. Gunturi, S. Shao, S. Konda, R.D. Buchner, M.T. Swihart, Flame-synthesized nickel-silver nanoparticle inks provide high conductivity without sintering, *Chem. Eng. J.* 372 (2019) 648-655.
- [8] S. Liu, M. Shah, S. Rao, L. An, M.M. Mohammadi, A. Kumar, S. Ren, M.T. Swihart, Flame aerosol synthesis of hollow alumina nanoshells for application in thermal insulation, *Chem. Eng. J.* 428 (2022).
- [9] M.M. Mohammadi, C. Shah, S.K. Dhandapani, J. Chen, S.R. Abraham, W. Sullivan, R.D. Buchner, E.A. Kyriakidou, H. Lin, C.R.F. Lund, M.T. Swihart, Single-Step Flame Aerosol Synthesis of Active and Stable Nanocatalysts for the Dry Reforming of Methane, *ACS Appl. Mater. Interfaces* (2021).
- [10] M.M. Mohammadi, S. Shao, S. Srivatsa Gunturi, A.R. Raghavan, N. Alexander, Y. Liu, C.M. Stafford, R.D. Buchner, M.T. Swihart, A general approach to multicomponent metal-decorated crumpled reduced graphene oxide nanocomposites using a flame-based process, *Nanoscale* 11 (2019) 19571-19578.
- [11] M.M. Mohammadi, A. Kumar, J. Liu, Y. Liu, T. Thundat, M.T. Swihart, Hydrogen Sensing at Room Temperature Using Flame-Synthesized Palladium-Decorated Crumpled Reduced Graphene Oxide Nanocomposites, *ACS Sens* 5 (2020) 2344-2350.